CURRENT CONTROLLED DC-DC CONVERTER FOR THE ENERGY STORAGE SYSTEM SOC MANAGEMENT

Miss MADASU LAYA[1], Mrs. A. Anuradha[2]
[1]*PG scholar in the Dept. of Electrical & Electronics Engineering, Holy Mary Institute of Technology & Science, Bogaram(V), Medchal District, Hyderabad, India.*
[2]*Assistant Professor in the Dept. of Electrical & Electronics Engineering, Holy Mary Institute of Technology & Science, Bogaram(V), Medchal District, Hyderabad, India.*

***Abstract*—** Abstract: A smart transformer (ST), which is a power electronic-based transformer with control and communication functionalities, can be the optimal solution for integrating a battery energy storage system (BESS) in an electric distribution system. In this paper, a unified current controller is introduced for a bidirectional dc-dc converter which employs complementary switching between upper and lower switches. The unified current controller is to use one controller for both buck and boost modes. Such a controller may be designed with analog implementation that adopts current injection control method, which is difficult to be implemented in high power applications due to parasitic noises. The averaged current mode is thus proposed in this paper to avoid the current sensing related issues. It has been shown that by sizing the BESS appropriately for the peak load demand, the power rating of ST converters can be reduced. The ST-based BESS provides an enhanced fault ride through capability, as compared to the conventional BESS. However, the state of charge (SOC) of the BESS shall be correctly managed to support the peak load demand when the ST converter reaches its maximum active power rating. Additional advantage with the unified digital controller is also found in smooth mode transition between battery charging and discharging modes where conventional analog controller tends to saturate and take a long delay to get out of saturation. The unified controller has been designed based on a proposed novel third-order bidirectional charging/discharging.

***Keywords*—** battery energy storage system (BESS), buck and boost modes, state of charge (SOC).

1. INTRODUCTION

The high power bidirectional dc-dc power converter has been widely used in hybrid electric vehicle and fuel cell applications [1-8]. To increase its power density, the design can adopt small inductor with multiphase interleaving to operate in discontinuous conduction mode (DCM) while reducing the ripples [9]. The problem with DCM operation is the related parasitic ringing caused by the inductor and the device output capacitance during current turn-off condition [9], resulting poor efficiency and significant EMI noises. A gate signal complementary control scheme was thus introduced to allow the inductor current continuously flow through the opposite direction such that the parasitic ringing is avoided, and the zero voltage soft switching (ZVS) is achieved [10]– [12]. This complementary switching scheme is also defined as "synchronous conduction" mode and is adopted here for a high-power bidirectional charger application. The combination of an electric grid, a DG, a BESS, and loads demands greater control and coordination to achieve maximum benefits while ensuring stable and reliable operation of the overall system. However, effective control and power management in such a complex system is limited with the today's conventional power transformer (CPT). The ST with the three-stage power converter architecture is a most suitable configuration for an electric distribution grid application [9].It has essential features of the CPT such as voltage transformation and isolation between a medium-voltage (MV) grid and a low-voltage (LV) grid and also provides features such as balanced sinusoidal voltages at its LV side, balanced sinusoidal currents at the MV side, and MV and LV dc links for integration of the different RES and storage [10]. The advantages of the ST in the electric grid have also been demonstrated through different operational features and ancillary services, for example, damping of LV grid resonance [11], better control and sharing of the power [12], var/volt control [13], a frequency adaptive ST in the LV grid [14], dc microgrid operation. The focus of this paper is to provide a detail procedure for selecting the different power converters of the ST while considering the peak load power demand and the maximum SOC availability of the BESS. With the

coordinated control of the load power demand, DG, and grid power, an effective SOC management is presented. An extensive analysis has been carried out to compare the charging/discharging efficiency and the reactive power injection capability of the ST-based BESS with the conventional BESS.

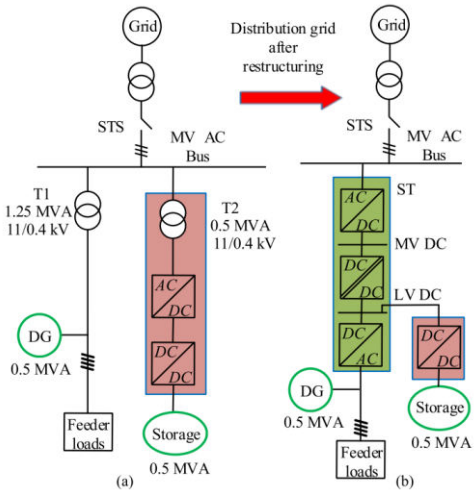

Fig. 1. Single-line diagram. (a) Conventional distribution electric grid. (b) Restructured distribution electric grid with transformer T1 is replaced by an ST, and the BESS is integrated into the LV dc-link of the ST.

One of the main switches takes care of both charging and discharging. This analog implementation relies on the competition of three error amplifiers, which tend to have difficulties in mode transition, because the error amplifier of the preferred mode is saturated during the transition [14].The analog implementation is also difficult to synchronize multiple phases. In this paper, a power stage averaged model is established based on the gate signal complementary control scheme. A unified digital controller, which essentially has the advantage of smooth mode transition capability due to the adoption of one main switch control and one common controller, both for battery charging and discharging thus is designed and implemented.

2. DESCRIPTION OF THE SYSTEM CONFIGURATION

ST-Based BESS Configuration

As shown in Fig. 1(b), a three-power-conversion-stage ST replaces the line CPT T1. The ac–dc stage of the ST, also called the ST rectifier, controls the MV grid side currents to ensure that the appropriate active power is exchanged while regulating the MV dc-link voltage around a reference voltage. The second stage is an isolated dc–dc converter, which converts MV dc to LV dc, provides an isolation between the MV and LV dc links, and regulates the LV dc link at a reference voltage. The third stage converter, the dc–ac converter or the ST inverter, maintains a constant balanced sinusoidal ac voltage at the LV side and supports the loads of line. The DG configuration remains the same in the proposed scheme. The LV dc link of the ST is utilized to integrate the BESS to the electric grid. A dc–dc converter is used to charge/discharge the battery bank. The MV dc and LV dc links of the ST are maintained at voltages of 30 and 1.2 kV, respectively. The battery specification remains the same as the conventional system.

3. SIZING OF DIFFERENT POWER CONVERTERS

The parameters of the conventional system configuration are given in Table I. In the proposed configuration, parameters given in Table II, both CPTs T1 and T2 are replaced by an ST. Also, the ac–dc converter of the BESS is eliminated. With the proper consideration of load demand and BESS capacity, an appropriate reduction in the sizing of the different power converters is also achieved.

A. Battery Bank and BESS

DC-DC Converter Under fully charged conditions, the BESS can supply 125-kW power continuously for 4 h. An averaged load profile, shown in Fig. 2, reveals that the average load demand is much lower than the rated power demand at most of the time of the day. The battery bank achieves its maximum SOC during day time by absorbing the DG power and supports the load during peak evening hours. Considering the SOC of the battery bank and the capability of continuously supplying the power, evening 4-h period is considered the peak load demand in this paper. The dc–dc converter is rated at 0.5 MVA to support the rated charging and discharging rate.

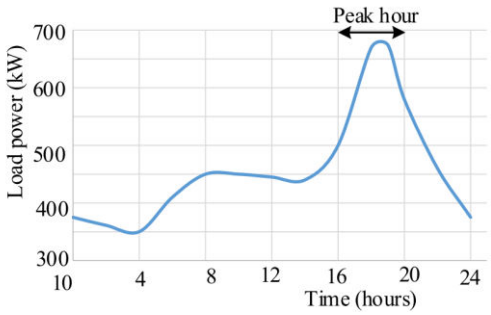

Fig. 2. Averaged load profile in a typical residential feeder [23]

B. Sizing of the ST Inverter

In the worst-case scenario when the DG output is zero, the inverter will completely supply the rated active, reactive, and harmonic powers of load. In this regard, the ST inverter power rating, Sinv−rated, is given as

$$S_{\text{inv}-\text{rated}} = \sqrt{P_{\text{l}-\text{rated}}^2 + Q_{\text{l}-\text{rated}}^2 + H_{\text{l}-\text{rated}}^2}$$

where Pl−rated , Ql−rated , and Hl−rated are rated active, reactive, and harmonic load powers, respectively. The load demand is kept the same in the proposed configuration, and therefore, the ST inverter of 1.25 MVA is selected.

C. Sizing of the ST DC–DC Converter

As already explained, the worst-case scenario is encountered when the DG power is zero during the rated load demand. In that case, the load power is shared by the BESS and the grid. During peak hours, let Pbess−peak be the power that the BESS supplies continuously. Therefore, the isolated dc–dc converter rating, Pdc−dc−rated, is given as

$$P_{\text{dc}-\text{dc}-\text{rated}} = P_{\text{l}-\text{rated}} - P_{\text{bess}-\text{peak}}$$

Here, Pl−rated is 0.7 MW and Pbess−peak is 0.125 MW. This requires the dc–dc converter of the ST to be rated for 0.575 MW.

D. Sizing of the ST Rectifier

The ST isolated dc–dc converter and the rectifier transfer the same active power at any given time, and therefore, the rectifier active power rating (Prec−rated) is the same as that of the isolated converter rating. However, the ST rectifier must also have a sufficient capability to support the reactive power similar to the conventional BESS. Let Qrec−rated be the ST-rectifier -rated reactive power compensation during the peak load conditions. Therefore, the ST rectifier apparent power rating will be

$$S_{\text{rec}-\text{rated}} = \sqrt{Q_{\text{rec}-\text{rated}}^2 + P_{\text{dc}-\text{dc}-\text{rated}}^2}$$

We consider that the ST has the capability to supply 0.3 MVAr into the MV grid when it exchanges rated active power with the grid. Therefore, the ST rectifier is rated for 0.65 MVA.

4. POWER FLOW IN THE PROPOSED ST-BASED BESS

Power flow for different operating modes is explained as follows.

Normal Operation (BESS Charging Done by the DG)

The load reactive and harmonic power is always supplied by the ST inverter. The active power flow depends upon the degree of availability of the DG and the load demand. In case 1, as shown in Fig. 3(a), DG power (PDG) is more than the active load power (Pl), and the battery bank is not fully charged. Therefore, rest of the power will be used for charging the battery bank. The ST rectifier and the DC–DC converter will not exchange power in this case (except the converter loss component). Once the battery bank is fully charged, this active power is injected into the MV grid through the rectifier and the dc–dc converter of the ST. The BESS converter draws power in this case. The corresponding power flow, as case II, is shown in Fig. 3(b). Fig. 3(c) shows power flow during case III when the DG power is not sufficient to meet the load power demand. In this situation, the load power deficit is supplied by the MV grid through the ST. As soon as the ST converters process rated power, the BESS is activated to supply the remaining power, as shown in Fig. 3(d).

5. REACTIVE POWER SUPPORT CAPABILITY

In addition to the active power support, the BESS in the conventional configuration also provides ancillary services in the MV distribution grid by appropriate injection of the reactive power. The ancillary services are realized by effective control of the active and reactive powers of the grid-side converter, which is limited by their fixed apparent power rating. Let S, P, and Q be the apparent power, the active power, and the reactive power exchanged by the power

converter with the grid, respectively, and these are related as follows:

$$S = \sqrt{Q^2 + P^2}$$

The capability curves for the conventional and proposed structures are shown in Fig. 7(a) and (b), respectively. It can be seen that in the ST-based BESS, a significantly large amount of reactive power can be injected into the grid compared to the conventional configuration. When the BESS charges/discharges at rated power, the proposed scheme has enough reactive power compensation capability as compared to negligible compensation capability in the conventional scheme

6. RELIABILITY OF THE PROPOSED SYSTEM

Conventional transformers have nowadays a very high reliability, which is still higher than a power-electronics-based solution. However, research on improving the reliability of actual solutions [10] as well as in improving the materials has already shown of improvement. Moreover, the implementation of fault-tolerant and repairable systems [32] is expected to further reduce the gap between the reliability of the CPT and the ST. If only the BESS is considered, then the proposed structure for charging/discharging uses a lower number of components as compared to the conventional BESS (a conventional BESS is realized using an AC–DC converter, a dc–dc converter, and a CPT, whereas the proposed scheme uses an AC–DC converter and a dc–dc converter). Considering that the CPT is highly reliable and both the schemes use equal number of power converters, the reliability of the BESS configuration can be assumed to be the same. However, when the proposed overall system is considered, more number of power converters are employed in comparison to the conventional CPT-based BESS, and therefore, presently, the reliability of the ST-based system will be lower than the CPT-based system.

7. OPERATION AND CONTROL

A. Control of the ST Rectifier

The rectifier draws active power requested from the MV grid to support the loads and also maintains MV dc-link capacitor voltage at a constant value. Moreover, it injects reactive power to provide ancillary services if needed. In this paper, reference currents of the rectifier are generated using instantaneous symmetrical component theory (ISCT) [33]. With the ISCT, the rectifier reference currents are given as follows:

$$i^*_{\text{rec}-a} = \frac{v^+_{ta1} + \frac{\tan\theta}{\sqrt{3}}(v^+_{tb} - v^+_{tc})}{(v^+_{ta1})^2 + (v^+_{tb1})^2 + (v^+_{tc1})^2}(P^*_{\text{rec}} + P_{\text{loss}})$$

$$i^*_{\text{rec}-b} = \frac{v^+_{tb1} + \frac{\tan\theta}{\sqrt{3}}(v^+_{tc} - v^+_{ta})}{(v^+_{ta1})^2 + (v^+_{tb1})^2 + (v^+_{tc1})^2}(P^*_{\text{rec}} + P_{\text{loss}})$$

$$i^*_{\text{rec}-c} = \frac{v^+_{tc1} + \frac{\tan\theta}{\sqrt{3}}(v^+_{ta} - v^+_{tb})}{(v^+_{ta1})^2 + (v^+_{tb1})^2 + (v^+_{tc1})^2}(P^*_{\text{rec}} + P_{\text{loss}})$$

where v+ ta1 , v+ tb1 , and v+ tc1 are fundamental positive-sequence point of common coupling (PCC) voltages in three phases at the MV side. The angle θ is a power factor angle responsible for reactive power injection. θ is the angle between active and reactive powers exchanged by the ST with the MV grid. For a reactive power demand of Q∗ rec, the power factor angle θ will be equal to tan−1 Q∗ rec P∗ rec+Ploss. Moreover, setting of θ = 0 will ensure that the reactive power is not exchanged from the MV grid. The power Ploss is the total power losses in the ST, and it helps in maintaining the MV dc-link voltage at a reference voltage. It is computed using a proportional–integral (PI) controller as follows:

$$P_{\text{loss}} = K_{p-\text{mv}}\, e_{\text{dc}-\text{mv}} + K_{i-\text{mv}} \int e_{\text{dc}-\text{mv}}\, dt$$

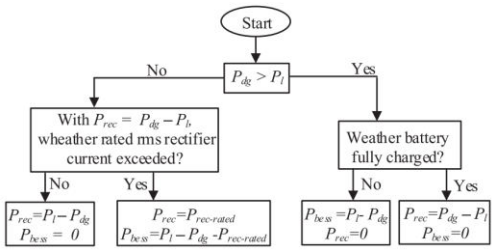

Fig. 9. Flowchart to select ST rectifier and BESS power.

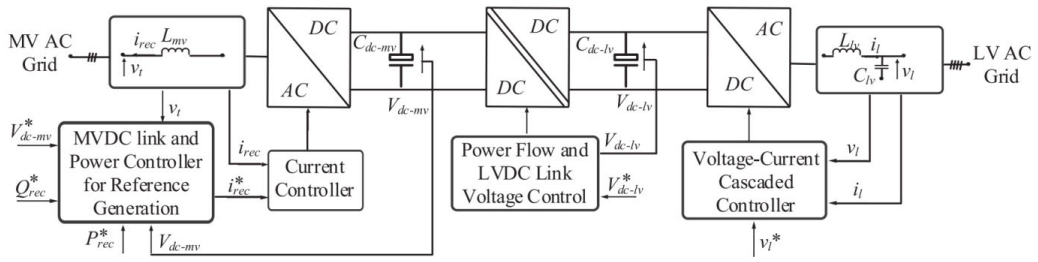

Fig. 8. ST control block diagram.

where Kp−mv, Ki−mv, and evdc−mv = V ∗ dc−mv − Vdc−mv are the proportional gain, the integral gain, and the voltage error of the PI controller, respectively. The parameters of the PI controller are tuned with the symmetrical optimum criterion [1]. The overall control block diagram of the ST is given in Fig. 8. In (8), the power P∗ rec is rectifier power requested from the grid. It will be different for different operating conditions, as shown in Fig. 9 and also explained as follows. Case I: If DG power is greater than load power and the battery is not fully charged, then rest of the power is used to charge the BESS. In this case, we have

$$P^*_{\text{rec}} = 0.$$

Case II: If DG power is greater than load power and the battery is fully charged, then rest of the power is send to the MV grid, i.e.,

$$P^*_{\text{rec}} = -(P_{\text{DG}} - P_l)$$

Case III: If DG power is lower than the load power requirement, then rest of the power is taken from the MV grid, provided that the rectifier does not reach its rated value, i.e.,

$$P^*_{\text{rec}} = P_{\text{DG}} - P_l$$

Case IV: Once the rectifier power reaches its rated value, i.e., P∗ rec = Prec−rated, then the deficit of the power is supplied by the BESS. This situation arises during peak load periods or during grid faults.

A. Control of the ST DC–DC Converter

This converter maintains the power balance between two dc links and regulates the LV dc-link voltage at a constant value.

The regulation of the LV dc link is achieved using a PI controller. The actual and reference LV dc-link voltages are compared to each other, and the error is passed through a PI controller having output as an angle φ

$$\phi = K_{p-\text{lv}}\, e_{\text{dc-lv}} + K_{i-\text{lv}} \int e_{\text{dc-lv}}\, dt$$

where Kp−lv, Ki−lv, and edc−lv = V ∗ dc−lv − Vdc−lv are the proportional gain, the integral gain, and the voltage error of the PI controller, respectively. φ is the angle between the pulsed voltages of two sides of the converter and ensures that the power flow is maintained between two dc links. The power transferred from one side of this converter to the other side is given as follows [16]:

$$P_{\text{dc-dc}} = \frac{V_{\text{dc-lv}} V_{\text{dc-mv}}}{2\pi f_{\text{sw}} L_{\text{dc-dc}}}\, \phi \left(1 - \frac{|\phi|}{\pi}\right)$$

where Ldc−dc is the leakage impedance of the high-frequency transformer, and fsw is the switching frequency of the converter. The converter power transfer characteristic is linearized around a constant value, and then, the symmetrical optimum criterion is implemented to achieve controller gains.

B. Control of the ST Inverter

The ST inverter maintains balanced sinusoidal voltages at the LV ac line having a magnitude of 230 V rms per phase and frequency of 50 Hz. At all the time of operation, it supplies for load reactive and harmonic powers. Active power transfer depends upon the DG power availability. If the DG power is more than the load power demand, then the additional power is fed back to the LV dc link by the inverter. However, the power is extracted from the MV grid and/or BESS in case DG power is not sufficient to meet the load demands. The control of the LV stage is cascaded voltage–current control. The inner current control based on a proportional regulator allows damping the resonance of the LC filter, whereas the outer PI control is used for the voltage control [1].

C. BESS SOC Control

In the power flow analysis, it has been seen that the battery bank can have four operating conditions: charging mode, discharging mode, fully charged mode, and not fully charged mode. The BESS dc–dc converter remains operational in the first two modes,

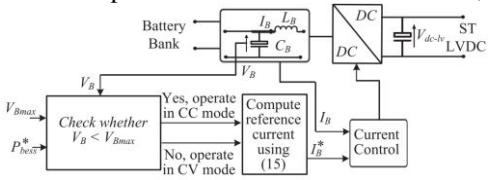

Fig. 10. BESS control block diagram.

The dc–dc converter of the BESS helps in maintaining the battery SOC within range during charging and allows us to support the loads during discharging. Let the power exchanges by the BESS be Pbess at any given time, and it can be given as follows:

$$P_{\text{bess}} = V_B I_B$$

where VB and IB are voltage across the battery bank and the current exchanged by the battery bank. As long as the voltage across the battery bank remains below the maximum value (VB max) during the charging, the BESS is operated in the constant current (CC) mode. Once the battery voltage reaches maximum set point values, the BESS is operated in the constant voltage (CV) mode [4]. Moreover, once the battery bank achieves the maximum SOC, the dc–dc converter is operated in floating charging mode to keep the battery bank fully charged. In this case, a small amount of current is taken to overcome the battery self-discharge. The control block diagram is shown in Fig. 10. The PI-based controller generates an angle δ, which is used to maintain the power balance [34]. Depending upon the different scenarios of the system configuration, the reference BESS power can be computed as follows.

Case I: DG power is greater than the load power demand, and the battery is not fully charged (battery SOC is smaller than SOCmax). In this case, the rest of the power is used to charge the BESS:

$$P^*_{\text{bess}} = P_{\text{DG}} - P_l.$$

Case II: DG power is greater than the load power demand, and the battery is fully charged (battery SOC is equal to SOCmax). In this case, the BESS will not exchange any power:

whereas in the last two modes, the converter remains in the standby mode. However, the converter must be able to switch between the different operational modes based on the control signal.

$$P^*_{\text{bess}} = 0$$

Case III: DG power is lower than the load power demand, and the power deficit is smaller than the ST rectifier power rating; then the BESS will not exchange any power:

$$P^*_{\text{bess}} = 0$$

Case IV: Once the rectifier power reaches its rated value, i.e., Prec = Precrated , then the deficit of the power is supplied by the BESS. This situation arises during peak load periods or during grid faults:

$$P^*_{\text{bess}} = P_l - P_{\text{DG}} - P_{\text{rec-rated}}$$

Control of the ST DC–DC Converter

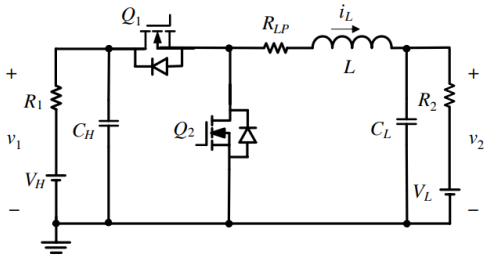

State-space averaging method is employed for the modeling of the bidirectional dc-dc converter with the following assumptions.

1. Current is relatively balanced among different phases. Thus simplified single phase is used for modeling.

2. Neglect dead time effect, since dead-time td is less than ten percent of switching period Tsw.

3. MOSFET turn-on resistance Rdson in both conduction directions is same.

4. The soft-switching period is neglected.

This converter maintains the power balance between two dc links and regulates the LV dc-link voltage at a constant value.

The regulation of the LV dc link is achieved using a PI controller. The actual and reference LV dc-l. The converter power transfer characteristic is linearized around a constant value, and then, the symmetrical optimum criterion is implemented to achieve

controller gains. link voltages are compared to each other, and the error is passed through a PI controller having output as an angle φ.With this ac model, the relationships between high side bus voltage v1, low side battery voltage v2, inductor current iL and duty cycle d are obtained. Since the buck charging and boost discharging current modes share the same power plant transfer function, they can share a unified controller. The defined inductor averaged current iL reference flow direction is the same as the battery charging power flow direction. it can be found that the current flow direction of IL only depends on the relationship between control duty cycle D and zero current duty cycle Do, which is defined in (9). To charge the battery, inductor averaged current IL should be greater than 0. According to (2), correspondingly duty cycle D should be adjusted to be greater than Do.

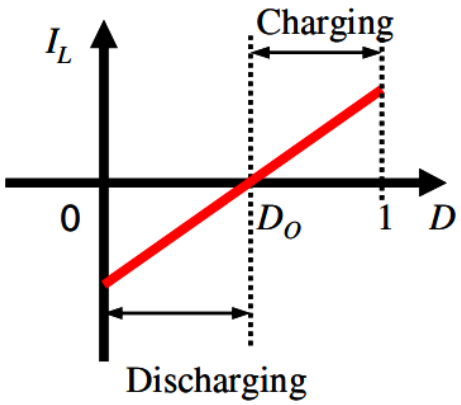

Duty cycle D versus inductor averaged current IL

8. SIMULATION RESULTS

The simulations are carried out in PSCAD software to show the performance of the proposed configuration during few operating conditions. It is considered that the battery bank is charged enough to support the loads. The first case is shown in Fig. 11. The MV grid voltage, ST rectifier currents, LV ac voltages, LV-side ST currents, and different active powers are shown in Fig. 11(a)–(e), respectively. The steady-state condition is shown from t = 1 to 2 s, where the load power demand is greater than DG power. In this case, the power deficit is supplied by the MV grid for maintaining power balancing. At t = 2 s, a voltage dip of 40% is created in the MV grid. If we consider the conventional BESS-based system, the overall BESS and the loads must be disconnected from the MV grid, while operating the overall system in the islanded mode. This operation again requires to be synchronized with the grid. Moreover, in the proposed configuration the system remains connected to the MV grid. The ST rectifier draws active power from the MV grid, depending upon the available rms current of the device. Once the rated current for the ST rectifier is reached, the remaining load power requirement is supplied by the BESS. It can be seen from figure that during the voltage dip, the ST current reaches its rated value to draw appropriate power. The BESS gets activated to support the rest load power requirement. Moreover, the DG power remains constant. Moreover, once the voltage is restored att = 3 s, the BESS power becomes zero, and the normal operation is restored. This feature of the proposed scheme allows the system to remain connected to the grid during voltage dips, which cannot be achieved in the conventional scheme. The second case, as shown in Fig. 12, provides the system performance during the peak load condition. It can be seen that the load power is 500 kW from t = 1 to 3 s, which is shared by the DG power and the MV grid. Moreover at t = 3 s, the load power changes to 675 kW. This power cannot be taken from the MV grid as the ST rectifier active power is limited to 575 kW. In this case, the ST rectifier currents increase to draw its rated power from the MV grid. The remaining power required by the load is supplied by the BESS. These waveforms are shown in Fig. 12. Moreover, once the loads are reduced at t = 5 s to the normal value, the control scheme detects that the load requirement can be met by the DG and the MV grid using ST power converters, and hence, the BESS power output slowly becomes zero.

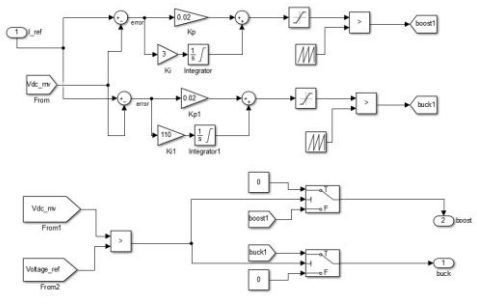

CURRENT CONTROLLER DC/DC BIDIRECTIONAL CONVERTER

The simulations are carried out in PSCAD software to show the performance of the proposed configuration during few operating conditions. It is considered that the battery bank is charged enough to support the loads. The MV grid voltage, ST rectifier currents, LV ac voltages, LV-side ST currents, and

different active powers. The steady-state condition is shown from t = 1 to 2 s, where the load power demand is greater than DG power. In this case, the power deficit is supplied by the MV grid for maintaining power balancing.

At t = 2 s, a voltage dip of 40% is created in the MV grid. If we consider the conventional BESS-based system, the overall BESS and the loads must be disconnected from the MV grid, while operating the overall system in the islanded mode. This operation again requires to be synchronized with the grid. Moreover, in the proposed configuration, the system remains connected to the MV grid. The ST rectifier draws active power from the MV grid, depending upon the available rms current of the device. Once the rated current for the ST rectifier is reached, the remaining load power requirement is supplied by the BESS. It can be seen from figure that during the voltage dip, the ST current reaches its rated value to draw appropriate power. The BESS gets activated to support the rest load power requirement. Moreover, the DG power remains constant. Moreover, once the voltage is restored at t = 3 s, the BESS power becomes zero, and the normal operation is restored. This feature of the proposed scheme allows the system to remain connected

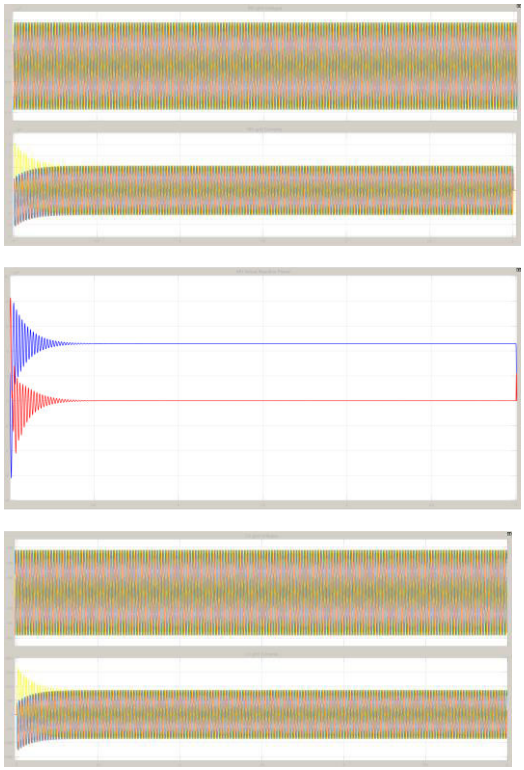

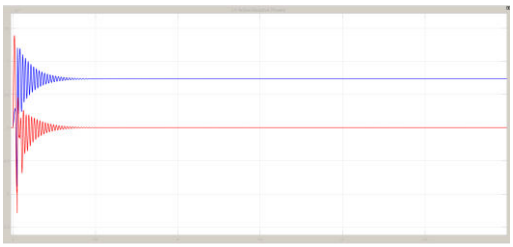

Fig. 11. Simulation results of the proposed configuration during voltage sag. (a) MV grid voltages. (b) ST rectifier current. (c) LV-side ST voltages. (d) LV-side ST currents. (e) Different active powers (normal operation for time interval T1 and T3 and operation during voltage sag for interval T2).

Fig. 12. Moreover, once the loads are reduced to the normal value, the control scheme detects that the load requirement can be met by the DG and the MV grid using ST power converters, and hence, the BESS power output is stable

CONCLUSIONS

The model contains voltage sources on both high- and low-sides and passive components. If both ends are constant voltage source. A unified averaged current mode controller, which controls only one duty cycle for both buck and boost modes, is designed based on the derived general-purposed model. The proposed Current controller is implemented to avoid mode transition discontinuity. Simulation results show that the proposed unified controller performs well in a high power bidirectional dc-dc converter. Stable operation is verified with load step up and down tests under both buck charging and boost discharging modes. In this paper, an ST was demonstrated as an effective solution for integrating the BESS in a distribution system. With effective control and SOC management, in addition to retaining the operational features of the conventional BESS configuration.

References

[1] R. Teodorescu, M. Liserre, and P. Rodriguez, Grid Converters for Photovoltaic

and Wind Power Systems, vol. 29. New York, NY, USA: Wiley, 2011.

[2] H. Rahimi-Eichi, U. Ojha, F. Baronti, and M. Y. Chow, "Battery management system: An overview of its application in the smart grid and electric vehicles," IEEE Ind. Electron. Mag., vol. 7, no. 2, pp. 4–16, Jun. 2013.

[3] C. S. Lai and M. D. McCulloch, "Sizing of stand-alone solar PV and storage system with anaerobic digestion biogas power plants," IEEE Trans. Ind. Electron., vol. 64, no. 3, pp. 2112–2121, Mar. 2017.

[4] T. V. Thang, A. Ahmed, C. i. Kim, and J. H. Park, "Flexible system architecture of stand-alone PV power generation with energy storage device," IEEE Trans. Power Convers., vol. 30, no. 4, pp. 1386–1396, Dec. 2015.

[5] J. von Appen, T. Stetz, M. Braun, and A. Schmiegel, "Local voltage control strategies for PV storage systems in distribution grids," IEEE Trans. Smart Grid, vol. 5, no. 2, pp. 1002–1009, Mar. 2014.

[6] J.-S. Lai, and D.J. Nelson, "Energy Management power converters in hybrid electric and fuel cell vehicles", in Proceedings of the IEEE, Vol. 95, No. 4, April 2007, pp. 766 – 777.

[7] D.P. Urciuoli and C.W. Tipton, "Development of a 90 kW bi-directional DC-DC converter for power dense Applications," in Proc. of IEEE APEC, Dallas, TX, Mar. 2006, pp. 1375–1378.

[8] P. Jose, N. Mohan, "A Novel Bidirectional DC-DC Converter with ZVS and interleaving for Dual Voltage Systems in Automobiles", in Conf. Rec. of IEEE IAS Annual Meeting, Oct. 2002, pp. 1311–1314.

[9] X. Huang, X. Wang, T. Nergaard, J.-S. Lai, X. Xu, L. Zhu, "Parasitic ringing and design issues of digitally controlled high power interleaved boost converters", IEEE Trans. Power Electron., Vol. 19, 2004, pp. 1341 - 1352.

[10] Y. Zhang, P.C. Sen, "A new soft-switching technique for buck, boost, and buck-boost converters," IEEE Trans. on IAS, Nov./Dec. 2003, pp.1775–1782.

Author's details

Miss MADASU LAYA received a diploma in Electrical and Electronics Engineering from Govt. Polytechnic Medchal College, Medchal, Medchal Malkajkiri (D), Telangana, India, and received a B.Tech degree in Holy Mary Institute of Technology and Science, Bogaram (V), Keesara (m), Medchal Malkajgiri (D), Hyderabad, Telangana, India from JNTUH University in 2021. And pursuing an M.Tech in Electrical Power Systems at Holy Mary Institute of Technology and Science, Bogaram (V), Keesara (M), Medchal Malkajgiri (D), Hyderabad, Telangana, India, in the Department of Electrical and Electronics Engineering.

Mrs. A. Anuradha received a B.TECH degree in EEE from Christu Jyothi Institute of Technology, Yeshwanthapur, Jangaon, Telangana, INDIA, from JNTU University and MTECH in Electrical Power Systems in Vignana Bharati institute of technology and sciences, near Ghatkesar Bogaram (v), Medchal Dist, Hyderabad, Telangana, INDIA. She has 2 years of teaching experience currently working as Assistant professor at Holy Mary Institute of Technology and Sciences, Bogaram, Medchal District, Hyderabad, Telangana, INDIA in the EEE department. His interest areas are Electrical power systems